ADVANCED FUNCTIONAL MATERIALS
www.afm-journal.de

Field Emission of Electrons Powered by a Triboelectric Nanogenerator

*Yunlong Zi, Changsheng Wu, Wenbo Ding, Xingfu Wang, Yejing Dai, Jia Cheng, Jiyu Wang, Zhengjun Wang, and Zhong Lin Wang**

Field emission of electrons usually requires high voltage (HV) of at least 100 V, which limits its applications due to the high cost, instability, portability issues, etc., of the HV instrument. Triboelectric nanogenerators (TENGs) have been developed to provide an HV of at least several kV for portable/mobile instrument, with controllability already demonstrated. Here, the field emission of electrons driven by TENG, namely, tribo-field emission, is presented for the first time. The emission voltage and the charge transfer per cycle can be tuned and controlled by TENG. The current peak generated from TENG with limited charge transfer is demonstrated to be more favorable than the direct current HV source in terms of emitter protection. A unidirectional continuous emission current is achieved through the tribo-field emission. A cathode-ray tube can be powered by TENG, with hours of illumination demonstrated through only one sliding motion. Such approach can provide a potential solution for controllable, stable, and portable field-emission devices without any additional external power sources.

1. Introduction

Field emission of electrons has been studied for over one century, which is related to the early research about electrons.[1–4] This phenomenon is now intensively involved in the technologies that require electron emissions, including but not limited to transmission electron microscopy, scanning electron microscopy (SEM),[5] and e-beam lithography.[6] Other applications with great commercial interests include field-emission display[7,8] (e.g., the field emission for cathode ray tube, CRT), microwave generation, X-ray generation,[9] charge neutralization, and nanoelectronics.[10,11] In recent decades, with the rapid development of nanotechnology, various nanostructured materials have been demonstrated for field emission through their field-enhancing effect at sharp tips and corners.[12–22] However, to satisfy the high electric field required for field emission, high voltage (HV) of at least 100 V is usually applied, which greatly limits the applications of field emission due to the high cost of HV instrument, limited controllability, stability concerns, and portability issues.

Triboelectric nanogenerator (TENG) is a low-cost emerging mechanical energy harvesting technology, which originates from the displacement current in the Maxwell's equations.[23–27] The mechanism based on the coupling effects of triboelectrification and electrostatic induction delivers unique output characteristics of TENG, including HV (usually over 1 kV) and low current/charge transfer. Therefore, applications of TENG on most of commercial electronics usually require complex power-management circuits/units to improve the overall efficiency.[28–31] However, this output from TENG can be directly used to drive HV applications, such as the electrospray process for mass spectrometry analysis,[32] air-particle removal,[33] and electrostatic actuation,[34–37] with the enhanced controllability demonstrated. As brought by TENG, this triboelectrification enabled HV can also create field emission of electrons, as called tribo-field emission.

Here, we presented the TENG-powered tribo-field emission for the first time. The emitter is fabricated by zinc oxide (ZnO) nanowire (NW) arrays grown on highly doped Si substrates. Field emissions driven by commercial HV source and TENG are demonstrated on the fabricated emitter, with the electric outputs carefully characterized. As driven by TENG, the voltage and the charge amount per cycle can be controlled precisely through the choice of the operation parameters, which can produce emission of electrons "as demanded." The limited amount of charge delivered by TENG can also prevent the ZnO nanostructures from exfoliating off from the substrate, which enhances the stability of the system. A unidirectional

Dr. Y. Zi, C. Wu, Dr. W. Ding, Dr. X. Wang, Dr. Y. Dai, Dr. J. Cheng, J. Wang, Dr. Z. Wang, Prof. Z. L. Wang
School of Materials Science and Engineering
Georgia Institute of Technology
Atlanta, GA 30332, USA
E-mail: zhong.wang@mse.gatech.edu
Dr. Y. Zi
Department of Mechanical and Automation Engineering
The Chinese University of Hong Kong
Shatin, N.T., Hong Kong SAR, China
Prof. Z. L. Wang
Beijing Institute of Nanoenergy and Nanosystems
Chinese Academy of Sciences (CAS)
Beijing 100083, China
Prof. Z. L. Wang
CAS Center for Excellence in Nanoscience
National Center for Nanoscience and Technology (NCNST)
Beijing 100190, China
The ORCID identification number(s) for the author(s) of this article can be found under https://doi.org/10.1002/adfm.201800610.

DOI: 10.1002/adfm.201800610

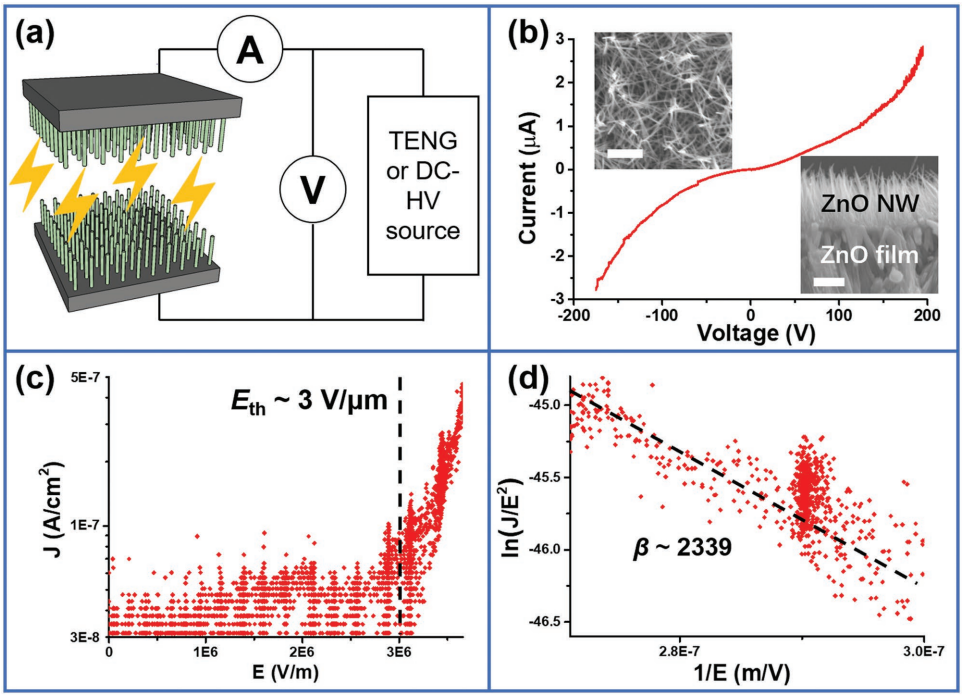

Figure 1. The fabricated emitter and the characterizations. a) The schematic diagram showing the emitter, the power source, and the measurement circuit. b) The measured *I*–*V* curve with SEM pictures of ZnO nanowires in top view (left up) and cross-sectional view (right down) as insets. Scale bars: 500 nm. c) The measured $\log_{10}J$–E curve showing the threshold electric field. d) The $\ln(J/E^2)$–$1/E$ curve showing the slope and the β value.

continuous field emission is achieved through rectifying circuits. The tribo-field emission display is demonstrated by a modified commercial CRT, with more than 100 min illumination achieved by only one sliding motion. Such results open a new era for the development of cost-effective, controllable, stable, and portable field-emission systems.

2. Results and Discussion

The setup for the field-emission measurement is shown in **Figure 1**a. The emitter is fabricated by two pieces of highly doped conductive Si substrates with grown ZnO NW arrays facing to each other. These ZnO NWs are hydrothermally grown on the predeposited ZnO film on the two Si substrates, each with an effective area of 1×1 cm^2. Through SEM, these NWs are characterized with <50 nm in the tip thickness and 1–2 μm in length (Figure 1b, inset). Kapton double-side tapes with thickness of 25 μm are used as spacers to separate the two substrates. This emitter is placed in a vacuum chamber with a pressure of $<10^{-6}$ torr. TENG or commercially available direct current (DC) HV source is connected to the backsides of the Si substrates to supply the HV required. The voltage and current/charge transfer are measured by electrometers separately.

By using the DC-HV power source, the measured voltage–current (*V*–*I*) curve of the fabricated emitter is shown in Figure 1b. As extracted from the curve between the current density J in the log scale and the applied electric field E in Figure 1c, the threshold field E_{th} is about 3 V μm^{-1}, which is similar to that from previous reports.[14,38–40] The emission characteristics can be explained by the Fowler–Nordheim equation as below[2,38,41]

$$J = \left(A\beta^2 E^2/\varphi\right)\exp\left(-B\varphi^{3/2}/\beta E\right) \quad (1)$$

here φ is the emission potential barrier, $A = 1.56 \times 10^{-10}$ A V^{-2} eV and $B = 6.83 \times 10^3$ V eV$^{-3/2}$ μm^{-1} are two constants, and β is the field enhancement factor brought by the nanostructured surface. As reported previously, ZnO material has a φ of ≈5.3 eV.[38–40,42] Based on this equation, the measured $\ln(J/E^2)$–$1/E$ curve is presented in Figure 1d. The measured dots with E slightly larger than E_{th} are fitted linearly as the dashed line, and through the fitted slope, $\beta \approx 2339$ is obtained. This β value is a little bit higher than previous reported values,[38–40,42] which might be attributed to the field-enhancing effect brought by the sharp tips of the grown NWs as shown in insets of Figure 1b.[22] These results validate the successful field emission from our fabricated ZnO NW based emitter.

To demonstrate the tribo-field emission, a freestanding sliding (FS) mode TENG is fabricated as shown in Figure S1a (Supporting Information), considering several advantages including its capability to produce HV, the controllability of the output, and the reliability. The operation mechanism of the FS-TENG has been reported in previous literature,[30,32,43,44] with the nylon (slider, usually 8×8 cm^2) and Teflon (stator) film as the positive and negative triboelectric surfaces, respectively. The fabricated FS-TENG is demonstrated to produce short-circuit charge transfer Q_{SC} of 400 nC (Figure S1b, Supporting Information). When this TENG is connected to a 1 nF capacitor, the voltage across the capacitor during TENG operation is measured by a Keithley 6514 electrometer as about

275 V (Figure S1c, Supporting Information). Considering this electrometer has a capacitance of 0.301 nF, the real open-circuit voltage V_{OC} is calculated as about 2600 V.[32] To double confirm the HV achieved by this TENG, a resistor with ultra-high resistance of 500 GΩ is connected to the TENG to approximate the open-circuit condition, and the current through this resistor is measured as inset in Figure S1d (Supporting Information). Through this method, the peak voltage across the resistor is measured to be close to 2500 V, (Figure S1d, Supporting Information) which validates the capability of the fabricated TENG to produce the HV output.

This TENG is used to power the tribo-field emission process. By connecting TENG to the emitter, with the voltage electrometer and a capacitor in parallel, the *I*–*V* curves as triggered by the TENG are measured, which are consistent with those measured using the DC-HV power source (**Figure 2**a,b). Here the voltage–charge transfer (*V*–*Q*) plot, which was proposed previously for TENG analysis and optimizations, is utilized to understand the operation cycle.[45,46] As shown in Figure 2c, in each half-cycle of the operation, there are three stages as marked by the numbers: in Step 1, the TENG charges the emitter like a capacitor, and there is negligible current leakage; in Step 2, when the voltage is over ≈100 V, the emission current becomes much larger, which induces a voltage plateau of about ≈200 V until the fully displacement of the slider being reached in TENG; in Step 3, the charge is fully released with the decreasing voltage and current. The other half-cycle operates similarly, with the negative voltage and the opposite charge transfer direction. The total transferred charge is about 400 nC.

Through the controlled operation of the TENG, the emission voltage and the charge transfer per cycle can be tuned. By operating TENG with only ≈40% of the original displacement, the total charge transfer is only ≈160 nC and the maximum absolute voltage can only achieve ≈150 V (Figure 2d). Through this method, the emission voltage and the charge transfer can

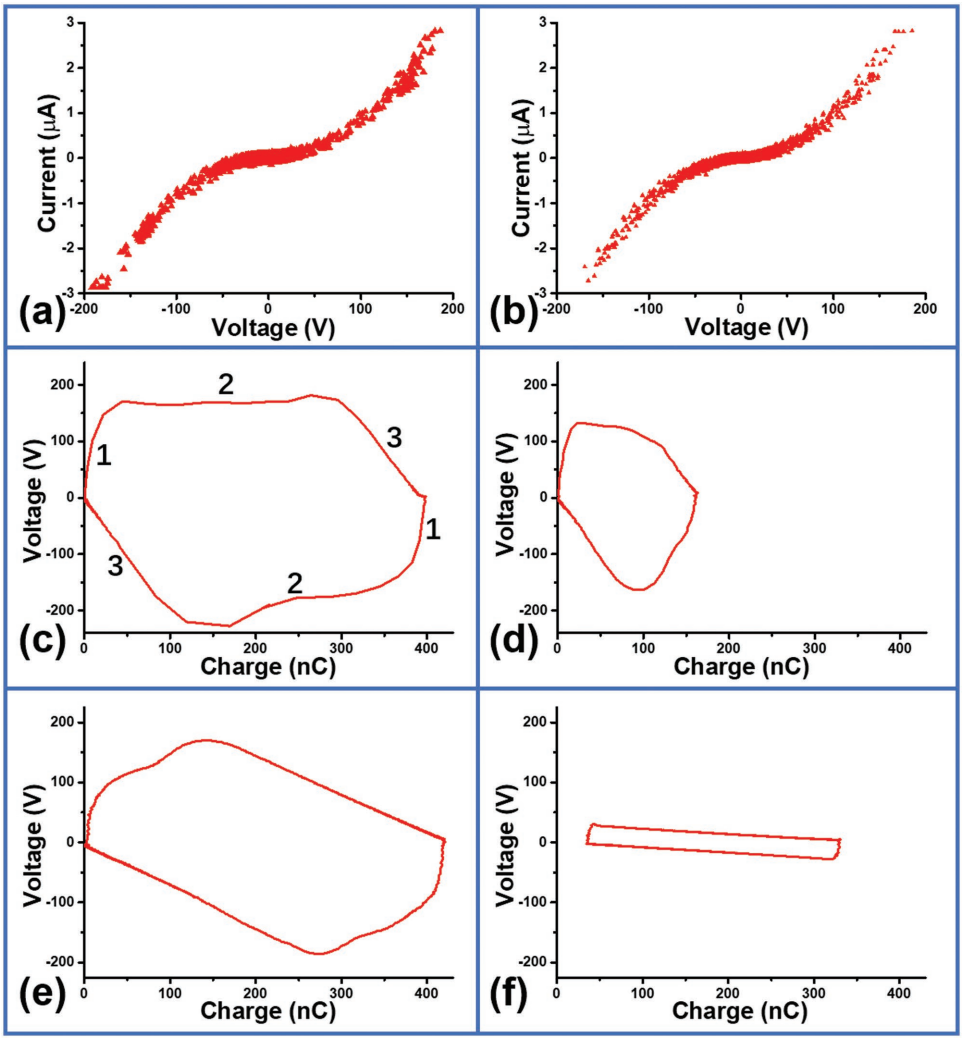

Figure 2. The operation performance of tribo-field emission. The *V*–*I* curves of the tribo-field emission with parallel capacitance of a) 0.301 nF and b) 1.301 nF. The *V*–*Q* plots with parallel capacitance of c) 0.301 nF, e) 1.301 nF, and f) 10.301 nF. d) The *V*–*Q* plots with parallel capacitance of 0.301 nF and only ≈40% displacement. Here the 0.301 nF is provided by the voltage electrometer, and even higher capacitance is supplied by additional capacitors in parallel.

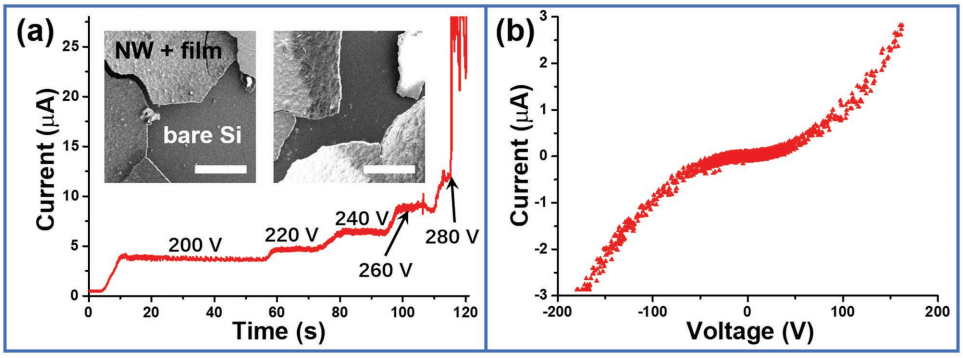

Figure 3. The safety test of the emitter under DC-HV and the TENG-HV. a) The current through the emitter with gradually increased voltage until ≈280 V. The insets show the exfoliated ZnO film with nanowires (NW) after test. Scale bars: 100 μm. b) The measured *V*–*I* curve after TENG-HV test, which is consistent with the previously measured curves.

be lowered simultaneously. By using additional capacitors in parallel, the total charge transfer keeps the same but the emission voltage decreases greatly. With an additional 1 nF capacitor in parallel, the maximum absolute voltage becomes about 160–180 V, while the charge transfer is maintained at about 400 nC (Figure 2e). However, if an additional 10 nF capacitor is connected, the voltage can only reach ≈30 V, which is not high enough to power the effective field emission (Figure 2f).

Another important concern is the stability of the emission current due to the damage of the emission surface. It has been observed for a while that various emission materials/structures can be destroyed during the field emission under HV.[47,48] This feature affects the long-term stability of the field emission. As tested in our study, by gradually increasing the voltage provided by the DC-HV source to be ≈280 V, the current suddenly increases with huge oscillations, as shown in **Figure 3**a. And then the voltage across the emitter cannot be maintained at the set point. This indicates that the original structure inside the emitter might be destroyed by the HV. As observed in SEM in the insets of Figure 3a, some parts of the ZnO film with NW structures are exfoliated from the Si substrates, which makes the two substrates electrically shorted at certain points. Since that the charge transfer per cycle is limited for TENG, it has been demonstrated that HV produced by TENG (TENG-HV) is safer for instrument.[32] Thus, TENG-HV is applied to the emitter to test its safety, and a partial voltage measurement method is used to estimate the peak voltage achieved (Figure S2a, Supporting Information). With a larger-area slider (9.5×10 cm^2), the peak voltage generated by the TENG can be pushed to be over 3000 V (Figure S2b, Supporting Information). And then, the *V*–*I* curve is measured, which is still consistent with the previously measured *V*–*I* curves (Figure 3b). This result indicates that the emitter is kept intact under the TENG-HV supply. In fact, even in the worst situation that a short circuit occurs, the safety will not be a concern for systems driven by TENG given its limited charge density.[49]

For most of applications, a continuous unidirectional output for the field emission is usually preferred. Here we design a circuit to achieve relatively stable voltage for tribo-field emission. The output of the TENG is first connected to a capacitor through a full-wave bridge rectifier, and then the emitter is connected in parallel with the capacitor (**Figure 4**a, inset). Therefore, the capacitor can supply a stable voltage output for the emitter, at the same time the charge consumption in the capacitor can be replenished by the TENG. One electrometer is connected in parallel to measure the voltage of the emitter, and the other one is connected in series to measure the current through the emitter. With a capacitor of 10 nC, the measured voltage and current are shown in Figure 4a,b, respectively, with the TENG operation frequencies of 1, 1.9, and 3 Hz. The variation of the unidirectional outputs can be decreased by simply using high-capacitance capacitors or batteries, which can maintain the output voltage in a relative small range. By using the capacitor with a higher capacitance of 68 nC, even more stable voltage and current are achieved with frequencies of 1.4, 2.8, and 4.1 Hz, as shown in Figure 4c,d. Hence, through this method, the unidirectional continuous tribo-field emission with over 100 V in voltage and several μA in current is achieved, and the output magnitude can be tuned by the operation frequency.

To demonstrate possible application of the tribo-field emission, we use TENG to power the field emission in a commercial CRT for display purpose. The schematic diagram of this CRT is shown in **Figure 5**a. There are three voltage inputs required for this CRT: the heating voltage (V_H) of 6–8 V is used to heat the filament; the wehnelt/focus voltage (V_W) of 10 V is for the focus adjustment of the electron beam; and the anode voltage (V_A) of 200–230 V is used for field emission of the electrons. The emitted electrons hit the inner surface with the fluorescent coating, and hence the interacted spot is illuminated to be green. Here V_H and V_W can be easily supplied by batteries, and the most difficult part is the HV power supply for V_A, which is provided by TENG in our experiment. As we demonstrated, the emission is enabled after only one sliding motion (corresponding to a half-cycle) as shown in Figure 5b and Video S1 (Supporting Information), while the next half-cycle operation with the reverse direction can turn the emission off as shown in Video S2 (Supporting Information). The voltage after triggering the tribo-field emission is measured as only about ≈210 V, (Figure 5c) which might be related to the threshold voltage set by the protection circuit inside the CRT. After a fully displacement of the slider in TENG to turn the emission on, through an instantaneously connected electrometer in short-circuit condition, the total charge release can be measured as ≈45 nC

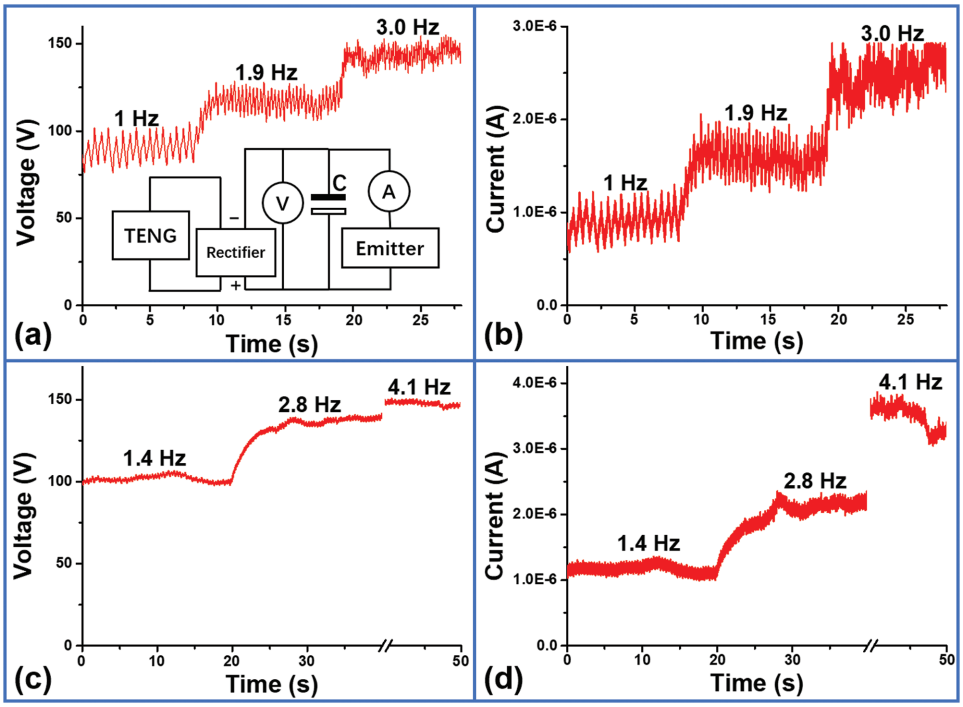

Figure 4. Continuous unidirectional tribo-field emission output. The a) voltage and b) current output achieved with a 10 nC capacitor and various frequencies. The circuit is shown in inset of (a). The c) voltage and d) current output achieved with a 68 nC capacitor and various frequencies.

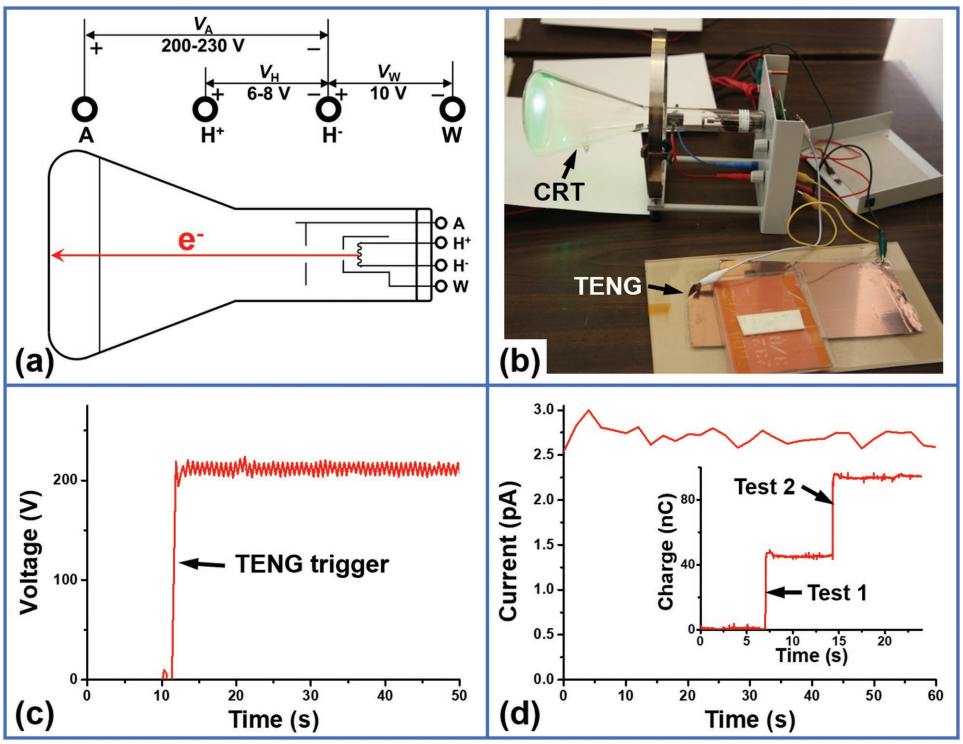

Figure 5. The tribo-field emission enabled CRT display. a) The schematic diagram of the CRT with required power supply. b) A photo showing successful display enabled by TENG. c) The measured voltage before and after the sliding motion. d) The measured emission current and the measured total charge release (twice) as inset.

(Figure 5d, inset). Therefore, the capacitance of this emitter is estimated as ≈0.21 nF. At the same time, the emission current is measured to be only about 2.5–3.0 pA, (Figure 5d) which means the electron emission can last for more than ≈100 min until the voltage is below the threshold emission voltage, as shown in Video S1 (Supporting Information) (see calculations in Note S1, Supporting Information). These results demonstrate a possible portable solution of CRT based on tribo-field emission for long-lasting-time display with minimum power consumption.

3. Conclusion

In summary, TENG has been demonstrated to supply HV to enable the tribo-field emission of electrons. The fabricated ZnO NW array based emitter is powered by TENG, with controllable voltage and charge transfer achieved. This approach is demonstrated to be more favorable than the DC-HV source in terms of emitter protection. The unidirectional continuous emission is enabled through rectifying circuits, with the emission voltage tuned by the operation frequency. The tribo-field emission is also demonstrated in a CRT for a portable, low-power, and long-lasting-time display. The tribo-field emission represents a potential solution for the next-generation low-cost field-emission instrument with enhanced controllability, stability, and portability.

4. Experimental Section

ZnO NW Array Growth: First, ZnO film as the seed layer was directly deposited on the highly doped silicon wafer (p-type (100), B doped, 1–10 Ω cm, from University Wafer) by radio frequency magnetron sputtering (PVD 75, from Kurt. J. Lesker Company) at the power of 100 W with the chamber pressure of 8 mTorr for 30 min. Then, the ZnO seed layer coated silicon wafer substrate was then placed into a mixed nutrient solution containing 25×10^{-3} M zinc acetate (from Alfa Aesar) and 25×10^{-3} M hexamethylenetetramine (from Alfa Aesar) for ZnO NW growth at 95 °C for 2 h in an oven. After cooling, the obtained sample was cleaned with deionized water and dried at 70 °C.

Fabrication of the Emitter for Field Emission: One piece of Si substrate was attached with double-side Kapton tape on the ZnO NW side as the spacer, confining a 1×1 cm^2 effective area. The other piece of Si substrate was attached with the ZnO NW side facing inside. The back sides of Si substrates were coated with silver paste and connected out as electrodes. To remove possible gases from the tape, the samples were left in the ultra-high vacuum for more than one day before measurements.

Fabrication of FS-TENG: The Teflon (fluorinated ethylene propylene) film was first deposited with copper film using PVD 75 system. A narrow tape was used as the mask to separate the deposited area into two parts as electrodes, each with area of 8.5×10 cm^2. The copper side of this Teflon film was attached on an acrylic board as the stator. Two sliders were fabricated by attaching nylon films on polyurethane foams and acrylic boards, with areas of 8×8 cm^2 and 9.5×10 cm^2. The materials were all purchased from McMasters.

Characterization Methods: The motions in most of experiments were triggered by hands, except the V_{OC} and Q_{SC} tests were conducted through a linear motor. The electrical measurements were mostly conducted by Keithley 6514 electrometers (with choices of voltage, current, and charge modes), except the ≈pA level current in Figure 5 was measured by a Keithley 4200 electrometer system. The measurement circuit for *V–Q* plot is as same as that for *V–I* plot as shown in Figure 1a, in which the electrometer for current measurement was set into charge mode for charge measurement. The commercial HV source is 3B Scientific U33000-230 DC Power Supply (0–500 V) purchased from Amazon. The CRT is 3B Scientific U8481350 Training Oscilloscope purchased from Amazon, with the function wave generator disconnected from the circuits to avoid consumption of charges.

Supporting Information

Supporting Information is available from the Wiley Online Library or from the author.

Acknowledgements

Y.Z., C.W., and W.D. contributed equally to this work. The research was supported by the Hightower Chair foundation, and the "Thousands Talents" program for pioneer researcher and his innovation team, China.

Conflict of Interest

The authors declare no conflict of interest.

Keywords

field emission, motion-controlled output, portable instruments, triboelectric nanogenerators

Received: January 24, 2018
Revised: March 4, 2018
Published online: April 6, 2018

[1] R. A. Millikan, C. F. Eyring, *Phys. Rev.* **1926**, *27*, 51.
[2] R. H. Fowler, L. Nordheim, *Proc. R. Soc. London, Ser. A* **1928**, *119*, 173.
[3] C. Kleint, *Prog. Surf. Sci.* **1993**, *42*, 101.
[4] C. Kleint, *Surf. Interface Anal.* **2004**, *36*, 387.
[5] A. V. Crewe, M. Isaacson, D. Johnson, *Rev. Sci. Instrum.* **1969**, *40*, 241.
[6] T. M. Mayer, D. P. Adams, B. M. Marder, *J. Vac. Sci. Technol., B: Microelectron. Nanometer Struct.—Process., Meas., Phenom.* **1996**, *14*, 2438.
[7] Q. H. Wang, A. A. Setlur, J. M. Lauerhaas, J. Y. Dai, E. W. Seelig, R. P. H. Chang, *Appl. Phys. Lett.* **1998**, *72*, 2912.
[8] M. Tanaka, K. Yano, *Patent number: US5838095A* **1998**.
[9] G. Z. Yue, Q. Qiu, B. Gao, Y. Cheng, J. Zhang, H. Shimoda, S. Chang, J. P. Lu, O. Zhou, *Appl. Phys. Lett.* **2002**, *81*, 355.
[10] P. H. Cutler, N. M. Miskovsky, P. B. Lerner, M. S. Chung, *Appl. Surf. Sci.* **1999**, *146*, 126.
[11] J.-W. Han, J. Sub Oh, M. Meyyappan, *Appl. Phys. Lett.* **2012**, *100*, 213505.
[12] W. A. De Heer, A. Chatelain, D. Ugarte, *Science* **1995**, *270*, 1179.
[13] S. Fan, M. G. Chapline, N. R. Franklin, T. W. Tombler, A. M. Cassell, H. Dai, *Science* **1999**, *283*, 512.
[14] S. H. Jo, J. Y. Lao, Z. F. Ren, R. A. Farrer, T. Baldacchini, J. T. Fourkas, *Appl. Phys. Lett.* **2003**, *83*, 4821.
[15] J. Zhou, N. S. Xu, S. Z. Deng, J. Chen, J. C. She, Z. L. Wang, *Adv. Mater.* **2003**, *15*, 1835.

[16] J. Chen, S. Deng, N. Xu, S. Wang, X. Wen, S. Yang, C. Yang, J. Wang, W. Ge, *Appl. Phys. Lett.* **2002**, *80*, 3620.
[17] Y. Zhu, T. Yu, F. Cheong, X. Xu, C. Lim, V. Tan, J. Thong, C. Sow, *Nanotechnology* **2004**, *16*, 88.
[18] Z. Pan, H.-L. Lai, F. C. Au, X. Duan, W. Zhou, W. Shi, N. Wang, C.-S. Lee, N.-B. Wong, S.-T. Lee, *Adv. Mater.* **2000**, *12*, 1186.
[19] J. Zhou, L. Gong, S. Z. Deng, J. Chen, J. C. She, N. S. Xu, R. Yang, Z. L. Wang, *Appl. Phys. Lett.* **2005**, *87*, 223108.
[20] J. H. He, R. Yang, Y. L. Chueh, L. J. Chou, L. J. Chen, Z. L. Wang, *Adv. Mater.* **2006**, *18*, 650.
[21] Y. D. Jiang, F. Zhang, C. J. Summers, Z. L. Wang, *Appl. Phys. Lett.* **1999**, *74*, 1677.
[22] P. G. Collins, A. Zettl, *Appl. Phys. Lett.* **1996**, *69*, 1969.
[23] F.-R. Fan, Z.-Q. Tian, Z. L. Wang, *Nano Energy* **2012**, *1*, 328.
[24] Z. L. Wang, *Mater. Today* **2017**, *20*, 74.
[25] Z. L. Wang, L. Lin, J. Chen, S. Niu, Y. Zi, *Triboelectric Nanogenerators*, Springer, Switzerland **2016**.
[26] Q. Liang, X. Yan, Y. Gu, K. Zhang, M. Liang, S. Lu, X. Zheng, Y. Zhang, *Sci. Rep.* **2015**, *5*, 9080.
[27] Q. Liang, Q. Zhang, X. Yan, X. Liao, L. Han, F. Yi, M. Ma, Y. Zhang, *Adv. Mater.* **2017**, *29*, 1604961.
[28] F. Xi, Y. Pang, W. Li, T. Jiang, L. Zhang, T. Guo, G. Liu, C. Zhang, Z. L. Wang, *Nano Energy* **2017**, *37*, 168.
[29] X. Cheng, L. Miao, Y. Song, Z. Su, H. Chen, X. Chen, J. Zhang, H. Zhang, *Nano Energy* **2017**, *38*, 438.
[30] Y. Zi, H. Guo, J. Wang, Z. Wen, S. Li, C. Hu, Z. L. Wang, *Nano Energy* **2017**, *31*, 302.
[31] S. Niu, X. Wang, F. Yi, Y. S. Zhou, Z. L. Wang, *Nat. Commun.* **2015**, *6*, 8975.
[32] A. Li, Y. Zi, H. Guo, Z. L. Wang, F. M. Fernández, *Nat. Nanotechnol.* **2017**, *12*, 481.
[33] C. B. Han, T. Jiang, C. Zhang, X. Li, C. Zhang, X. Cao, Z. L. Wang, *ACS Nano* **2015**, *9*, 12552.
[34] X. Chen, Y. Wu, A. Yu, L. Xu, L. Zheng, Y. Liu, H. Li, Z. Lin Wang, *Nano Energy* **2017**, *38*, 91.
[35] L. Zheng, Y. Wu, X. Chen, A. Yu, L. Xu, Y. Liu, H. Li, Z. L. Wang, *Adv. Funct. Mater.* **2017**, *27*, 1606408.
[36] X. Chen, X. Pu, T. Jiang, A. Yu, L. Xu, Z. L. Wang, *Adv. Funct. Mater.* **2017**, *27*, 1603788.
[37] X. Chen, T. Jiang, Y. Yao, L. Xu, Z. Zhao, Z. L. Wang, *Adv. Funct. Mater.* **2016**, *26*, 4906.
[38] C. X. Xu, X. W. Sun, *Appl. Phys. Lett.* **2003**, *83*, 3806.
[39] C. J. Lee, T. J. Lee, S. C. Lyu, Y. Zhang, H. Ruh, H. J. Lee, *Appl. Phys. Lett.* **2002**, *81*, 3648.
[40] X. D. Wang, J. Zhou, C. S. Lao, J. H. Song, N. S. Xu, Z. L. Wang, *Adv. Mater.* **2007**, *19*, 1627.
[41] R. G. Forbes, *J. Vac. Sci. Technol., B: Microelectron. Nanometer Struct.—Process., Meas., Phenom* **2008**, *26*, 788.
[42] Y. K. Tseng, C. J. Huang, H. M. Cheng, I. N. Lin, K. S. Liu, I. C. Chen, *Adv. Funct. Mater.* **2003**, *13*, 811.
[43] S. Niu, Y. Liu, X. Chen, S. Wang, Y. S. Zhou, L. Lin, Y. Xie, Z. L. Wang, *Nano Energy* **2015**, *12*, 760.
[44] S. Wang, Y. Xie, S. Niu, L. Lin, Z. L. Wang, *Adv. Mater.* **2014**, *26*, 2818.
[45] Y. Zi, L. Lin, J. Wang, S. Wang, J. Chen, X. Fan, P.-K. Yang, F. Yi, Z. L. Wang, *Adv. Mater.* **2015**, *27*, 2340.
[46] Y. Zi, J. Wang, S. Wang, S. Li, Z. Wen, H. Guo, Z. L. Wang, *Nat. Commun.* **2016**, *7*, 10987.
[47] A. L. Koh, E. Gidcumb, O. Zhou, R. Sinclair, *Nanoscale* **2016**, *8*, 16405.
[48] Z. Xu, X. D. Bai, E. G. Wang, Z. L. Wang, *Appl. Phys. Lett.* **2005**, *87*, 163106.
[49] Y. Zi, C. Wu, W. Ding, Z. L. Wang, *Adv. Funct. Mater.* **2017**, *27*.